Adsorption of Copper (II) IonsIn Aqueous Solution Using Bio- synthesized Nanocomposite From Avocado Pear Seed.

ABSTRACT

This study uses avocado peer seed and silver metal nanocomposite made from avocado peer seed to investigate the adsorption capability of copper (II) ions from aqueous solution. The agro waste underwent treatment processes such as chemical, physical and hydrothermal synthesis giving rise to a nanocomposite with an enhanced surface area, structure and functional groups. In the investigation of the adsorption capacity of copper (II) ions, numerous factors were examined, including pH, concentration, dose, temperature, and contact time. Assessments were also conducted on the kinetic data, equilibrium isotherm, and thermodynamics investigations. To clarify the functional group, shape, and crystalline size of the avocado peer seed and the silver-synthesised avocado peer seed adsorbent, FTIR, SEM, and XRD analysis were used. Langmuir and Freundlich adsorption models were employed in the characterization of the adsorption equilibrium isothers. It was determined that the Langmuir adsorption model provided a better fit to the experimental data compared to the Freundlich models.

Keywords: Adsorption, Avocado peer seed (APS), Copper, Silver metal nanocomposite (AgAPS)

1.0 INTRODUCTION

The use of science to manipulate matter at the molecule level is known as nanotechnology. Research on nanotechnology has been established since the turn of the century, and there have been some groundbreaking advancements in this area. Materials at different nanoscale levels are produced using nanotechnology. According to Laurent *et al*., (2010), nanoparticles (NPs) are a broad class of materials that comprise particulate compounds with a minimum size of less than 100 nm. Every area of medicine has become more interested in NPs because of their capacity to administer medications within the ideal dosage range, which frequently boosts the therapeutic efficacy of the medications, reduces their adverse effects, and increases patient compliance (Alexis *et al*., 2008).For biomedical applications, iron oxide particles like magnetite (Fe_3O_4) or its oxidized counterpart, maghemite (Fe_2O_3), are most frequently used (Ali *et al*., 2016). Metal precursors are the only material that makes up metal nanoparticles. These NPs have distinct opto-eletrical features because of their well-known localized surfaces Plasmon resonance (LSPR) characteristics. Ag and Au, two alkali and noble metal NPs, have wide absorption spectra. In today's cutting edge materials, the facet, size, and shape controlled production of metal nanoparticles is crucial (Dreaden *et al*., 2012). The avocado plant, *Persea americana*, is a member of the Lauraceae family and genus. It produces fruit that is sometimes referred to as alligator pears or avocado pears, and it includes avocado pear seeds. Avocado pear seed has been reported to be used to treat inflammation, diabetes, cancer, and hypertension (Adeyemi *et al*., 2002; Anaka *et al*., 2009; Ojewole and Amabeoku, 2006). In Ojoto and the surrounding Igbo-speaking villages in southeast Nigeria, the fruit is referred to as ube oyibo, which roughly translates to "foreign pear" (Egbuonu*et al*., 2017). Alhassan *et*

al.,(2012)reported that the avocado pear was utilized in traditional medicine for a variety of purposes, including as an antibacterial medicament.On the other hand, mining, industrialization, and agriculture have all contributed to an increase in NPs, or heavy metal, pollution of the environment (Dahiya *et al*., 2008). Metallurgical and electroplating activities transfer hazardous heavy metals into wastewaters from industry, contaminating drinking water sources (Huang and Zhi-min, 2013). Both humans and animals can and do experience major consequences from these contaminants. Industrial wastewater frequently contains heavy metal ions, such as Cu(II), Cd(II), Pb(II), and As, which can be acutely harmful to aquatic and terrestrial life. Cu(II) has also been reported to accumulate in food, particularly in liver, shellfish, nuts, and mushrooms. Cu(II) contamination can also occur in food. Adsorption using biomass is one of the most popular and effective processes for the removal of heavy metals from wastewaters. To address the issues posed by the use of these conventional sorbents, nanomaterials have been investigated as material to enable efficient removal of heavy metal ions from wastewater (Hua *et al*., 2012). Conventional methods that have been used to remove heavy metal ions from various industrial effluents usually include chemical precipitation, membrane separation, ion exchange, evapouration, electrolysis, etc. These are often costly, non biodegradable, or ineffective in the removal of heavy metal ions from wastewaters; therefore, the removal of these heavy metal ions from wastewaters before discharging into clean water bodies is of importance.Methods for creating nanoparticles include thermal decomposition in organic solvents (Esumi*et al*., 1993), chemical reduction and photoreduction in reverse micelles (Pileni, 2001), and chemical reduction of the metal ions in aqueous solutions with or without stabilizing agents (Liz – Marzan and Lado – Tourina, 1996). The majority of these techniques are pricey. The contamination of heavy metal ions affects all elements of the ecosystem, including the air, water, and soil (land). Heavy metal ion pollution of land can result from several activities, including but not limited to industrial processes, mining tailings, high metal ion content waste disposal, and fertilizer application on land, sewage sludge pesticides, crude oil, and petrochemical operations. Heavy metal absorption by plants typically has an impact on the yield and productivity of the product, which in turn has an impact on the nation's economy and food production. Runoff from cities and industries has an impact on water bodies as well (Radhakrishnan *et al*., 2015). Natural processes like rock weathering, volcanic eruptions, and soil erosion can all contribute to air pollution (Ventura *et al*., (2017).Therefore removal of heavy metal ions in effluents remains imperative to mitigate the above problems as this research aims at investigating the equilibrium kinetic and thermodynamic studies for the adsorptive removal of copper ion using biosynthesized nanocomposite by biosynthesizing silver nanocomposite using *Persea americana* seed, characterizing the biosynthesized copper nanocomposite, carry out equilibrium kinetics and thermodynamic studies using the biosynthesized nanocomposite in the removal/ adsorption of Cu(II) ion and determine the mechanism of adsorption of the Cu(II) on the silver metal nanocomposite using Langmuir, Freundlich adsorption isotherms.

2.0 Methods

2.1 Preparation of the agro waste

The avocado pear seed was collected from Achina, in Aguata L.G.A of Anambra State. Nigeria. They were washed with distilled water, allowed to dry away from direct sunlight and ground into powder, then subjected to a 48-hour extraction process at room temperature using methanol as the solvent. Subsequently, the extracts utilizing Whatman No.1 paper, resulted in an extraction of crude extracts subsequent to concentration under reduced pressure (Djeussi*et al*.,2020).

2.2 Synthesis of Silver Nano Composites

1M $AgNO_3$ solution was prepared by simply dissolving $AgNO_3$ flakes with distilled water. Samples of the avocado pear seed extract were added to the $AgNO_3$ solution. The combination was subjected to incubation at ambient temperature until the yellow hue of the solution transitioned to a deep brown shade. The samples were then centrifuged for 20 minutes at 5000 revolutions per minute, and the supernatant was disposed of after the process. A volume of 5 mL of deionized water was introduced to the precipitate, followed by another round of centrifugation under identical conditions. The procedure was replicated. Subsequently, the ultimate precipitate was subjected to a temperature of 60°C in a hot air oven for a duration of 30 minutes (Naveed *et al.,* 2022).

2.3 Preparation of Stock Solutions (Adsorbate)

Distilled water was used throughout the experiment to dilute copper chloride dehydrate (≥ 99% purity) obtained from the chemical shop. All solutions used in the experiment were prepared in double distilled water. Stock solution of the test reagent was made by dissolving 1000mg of copper dehydrate (≥ 99% purity) in one liter of distilled water. The stock solution underwent dilution in order to get various quantities of copper ions that were necessary for conducting the tests.

2.4. Characterization of Adsorbents

2.4.1. Fourier Transform InfraRed Spectroscopy (FTIR)

The Fourier Transform InfraRed (FTIR) Spectrophotometer was employed to ascertain the functional groups present in the samples(Naveed *et al.,* 2022).

2.4.2. Scanning Electron Microscope (SEM) Analysis

SEM was used to ascertain the structural characteristics of the nanocomposite acquired. The dried samples were affixed to a sample holder using double conductive tape at room temperature. To enhance conductivity, a layer of platinum-gold coating was administered onto the samples. Subsequently, the samples were subjected to visualization using an 80 kV voltage (Naveed *et al.,*2022).

2.4.3. X-ray Diffraction (XRD) Analysis

X-ray diffraction (XRD) was employed to analyse the crystalline nature of the AgNPs. The experiment employed a powdered material, and the scanning mode was conducted using a current of 30 mA, a voltage of 40 kV, and Cu/Kα radiation. The diffraction pattern was then recorded within the 2θ angle range of 20^0C–70^0C.

The scherrer equation was used to determine the particle size and is giving by

$$D = \frac{K\lambda}{\beta Cos\theta} \quad 2.1$$

Where D is the nanocomposite crystalline size, K represents the Scherrer constant (0.98), λ denotes the wavelength(1.54), β denotes the full width at half maximum (FWHM).

2.5. Batch Adsorption process

The batch experiments were performed using adsorbent material placed in Erlenmeyer flasks, which were sealed with glass stoppers to minimize evaporation. The mixtures were stirred using a mechanical magnetic stirrer operating at a speed of 200 revolutions per minute. The objective was to determine the optimal conditions in terms of pH, adsorbent type, and lead(II) ion concentrations.

2.5.1. Effect of pH

In order to determine the effect of pH on the adsorption of copper(II) ions onto Avocado pear silver nanocomposite, the adsorption mixture was brought into equilibrium with a 20 ml solution containing 150 mg/dm^{-3} of copper(II) ions and dried adsorbent. The experiment was conducted at pH levels of 2, 4, 6, 8, and 10. The pH was adjusted by employing 0.1 M hydrochloric acid (HCl) and 0.1 M sodium hydroxide (NaOH) solutions. The experiment involved the regulation of the adsorbent quantity to 0.1g, the temperature to 30^0C, and the duration to 60 minutes.

2.5.2. Effect of adsorbent dosage

The impact of adsorbent dose was investigated by manipulating the weights of the Nano composites within the range of 0.1g, 0.2g, 0.3g, 0.4g, and 0.5g. Subsequently, these samples were subjected to testing under the specified experimental circumstances. The experimental conditions included a duration of 60 minutes, a temperature of 300°C, a pH value of 6, and a concentration of 150 mg/L.

2.5.3. Effect of time

The study investigated the impact of time by manipulating the duration at intervals of 30 minutes, namely at 30, 60, 90, 120, 150, and 180 minutes. These variations were examined under the specified experimental settings. The experimental conditions included a temperature of 300°C, a pH value of 6, a dosage of 0.1g, and a concentration of 150 mg/L.

2.5.5. Effect of Temperature

The study investigated the impact of temperature by manipulating the duration at intervals of 5^oC, namely at 30, 35, 40, 45 and 50^OC. These variations were examined under the specified experimental settings. The experimental conditions included a pH value of 6, a dosage of 0.1g, and a concentration of 150 mg/L.

2.5.6. Effect of initial metal ion concentration

The impact of the initial metal ion concentration was investigated by manipulating concentrations at 100 mg/L, 150 mg/L, 200 mg/L, 250 mg/L, and 300 mg/L under the specified experimental settings. The experimental conditions included a time duration of 60 minutes, a dosage of 0.1g, a temperature of 300°C, and a pH level of 6.The metal solutions' concentrations were determined using atomic absorption spectroscopy, specifically utilizing the AA500F Atomic absorption spectrophotometer. Additionally, a control experiment was conducted utilizing identical solution and equipment, with the exception of the nano-composite adsorbents.

2.5.5. Adsorption Capacity

The experimental adsorption capacity (qe mg/g) after equilibrium was calculated as follows:

$$q_{e=(C_0 - C_e)\frac{V}{m}} \quad 2.2$$

Where Co and Ce are the initial and equilibrium concentration (mg/L) of Pb respectively. "V" is the volume of the solution and "m" is the amount of adsorbent.

$$E\% = \frac{(C_0 - C_e)}{C_0} x\ 100 \quad 2.3$$

Where E is the Adsorption capacity.

2.6 Kinetic Studies

The kinetic studies was carried out with different concentrations (10mg L^{-1} , 20mg L^{-1}, 30mg L^{-1}) of solutions at room temperature (300K) in contact with the optimum dosage prepared nanoparticle (adsorbent). Samples of Cu(II) were removed at different time intervals (20 to 100min) and the metal concentration was measured. The metal uptake was calculated using kinetic equations. The sorption kinetic data of Cu(II) on the adsorbent was analysed in terms of pseudo first order and pseudo second order sorption equations. The pseudo first order equation was first suggested by Lagergren and the equation is below.

2.7 Equilibrium Isotherm Models

Investigating the adsorption isotherm, two models were used. The Langmuir and the Freundlich.

Isotherm plots were drawn from the experimental data of the amount of Cu(II) adsorbed per unit mass (mg g^{-1}) versus equilibrium solution concentration for the adsorption of Cu(II).

2.8 Thermodynamic studies

Thermodynamic equations were employed to determine the spontaneity of adsorption and to investigate the impact of temperature on the adsorption process. The calculation of the equilibrium constant, Kc, relies on equation (2.5). Consequently, the thermodynamic equation can be expressed in a linear form, known as the van't Hoff isotherm equation, as depicted in equation 2.4.

$$\Delta G = -RTlnk_C \quad 2.4$$

$$lnk_C = \left(\frac{C_A}{C_e}\right) \quad 2.5$$

$$lnk_C = \left(\frac{-\Delta H}{R}\right).\frac{1}{T} + \left(\frac{\Delta S}{R}\right) \quad 2.6$$

3.0 RESULTS AND DISCUSSION

3.1 Infrared Spectroscopic Studies

Infrared Spectroscopic Studies for avocado pear seed (APS) and Silver Oxide nano-particle-Avocado Pear Seed (AgAPS)

The FTIR spectrum of APS and AgAPS and the observed signals are presented below:

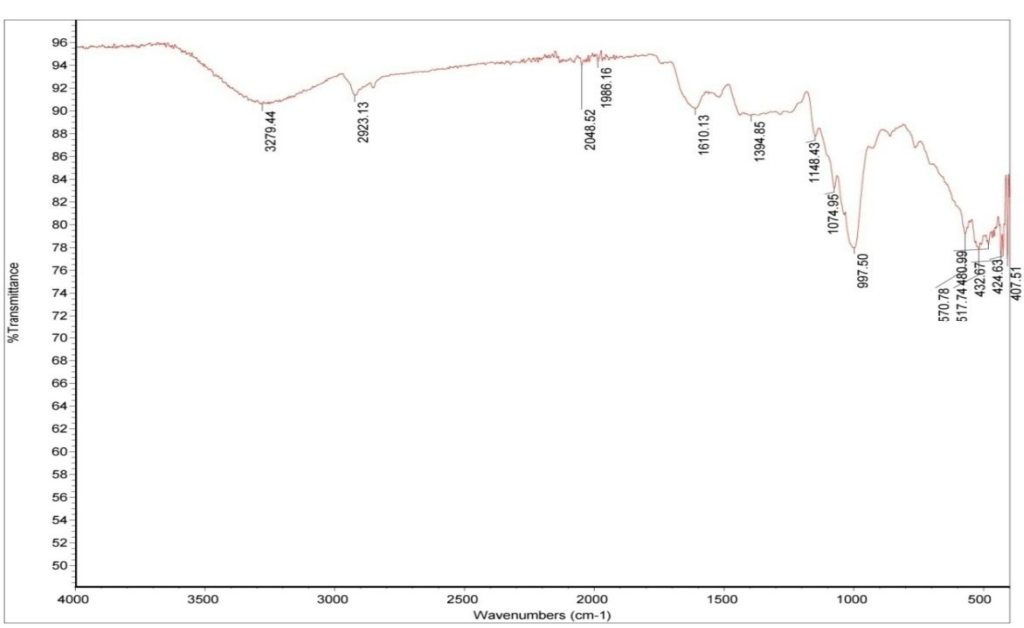

Fig 1. Infrared Spectroscopic Spectrum for avocado pear seed (APS)

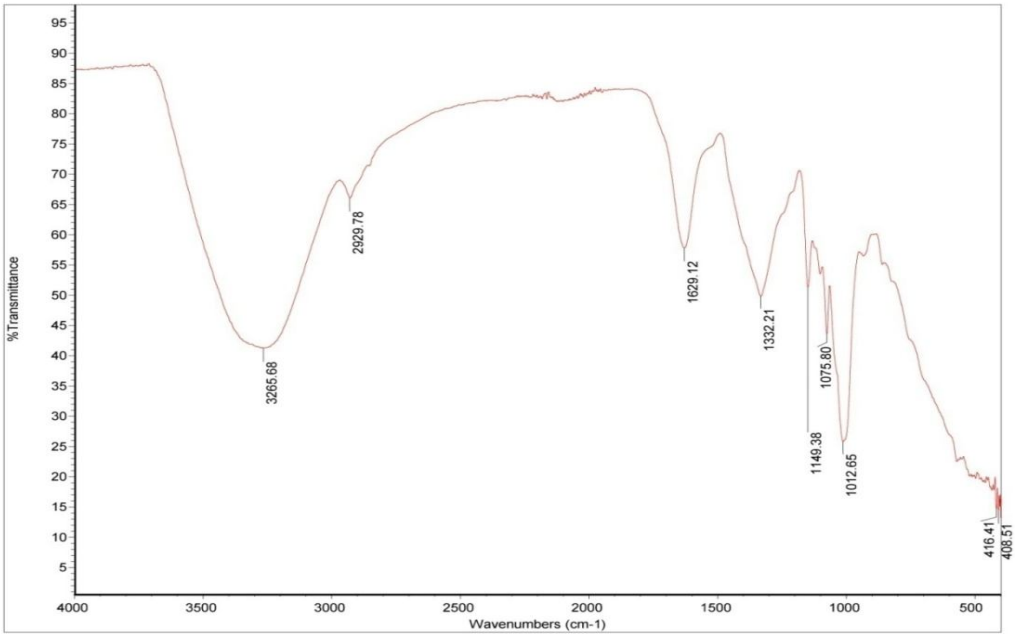

Fig 2. Infrared Spectroscopic Spectrum of Silver Oxide nano-particle-Avocado Pear Seed (AgAPS)

Table 1-Assignments of the IR spectra bands of functional groups in APS and AgAPS

APS band positions (cm^{-1})	AgAPS band positions (cm^{-1})	Proposed signal group
3279	3265	OH stretching
2923	2929	CH stretching
2048 and 1986	-	C≡C of alkynes
1610	1629	C=O stretching
1394	1332	C-H bending
1148	1149	C-O stretching
1074	1076	C-O stretching

After impregnation of silver oxide nano-particles (AgNOPs) onto APS, shifts were observed in the absorption bands of the OH group from 3279 to 3265cm-1, the C-H bands from 2923 to 2929 cm-1, the C=O bands from 1610 to 1629cm-1, the C≡C bands completely disappeared. This shows the interaction of the impregnated AgONPs with the surface functional groups on the APS surface. In addition, the presence of surface functional group on both the APS and AgAPS sorbents, indicates the potential of the prepared sorbents to remove pollutants from aqueous medium. This is in agreement with (Akpomie and Conradie, 2020b).

3.2 XRD Characterization

XRD Spectroscopic Studies for avocado pear seed (APS) and Silver Oxide nano-particle-Avocado Pear Seed (AgAPS)

The XRD spectra provides information on the crystal phase of the Sorbents as shown in Figure 3 for APS, the cellulose diffraction at 2θ of 15^0, 17^0, 27^0 and 31^0 is characteristics of agrowaste (Dai *et al*; 2020). For AgAPS as shown in Figure .4, the face centred cubic structure of Ag nanoparticle was confirmed by 2θ diffractions at 38^0, 44^0, 65^0 and78^0 corresponding to (111), (200), (220) and (311) Ag reflections respectively. This proves the presence of similar nanoparticles on the AgAPS composites. Similar diffractions were obtained for Ag nanoparticles synthesized from the seed extract of Alpina Kat Sumodai as reported by (He *et al*, 2017).

The scherrer equation was employed in figure 4 to determine the particle size of the higher peaks in the spectra. The 2θ diffractions at the 5 highest peak, 15^o, 17^0, 39^0, 65^0 and 78^0 has an average particle size of 95nm

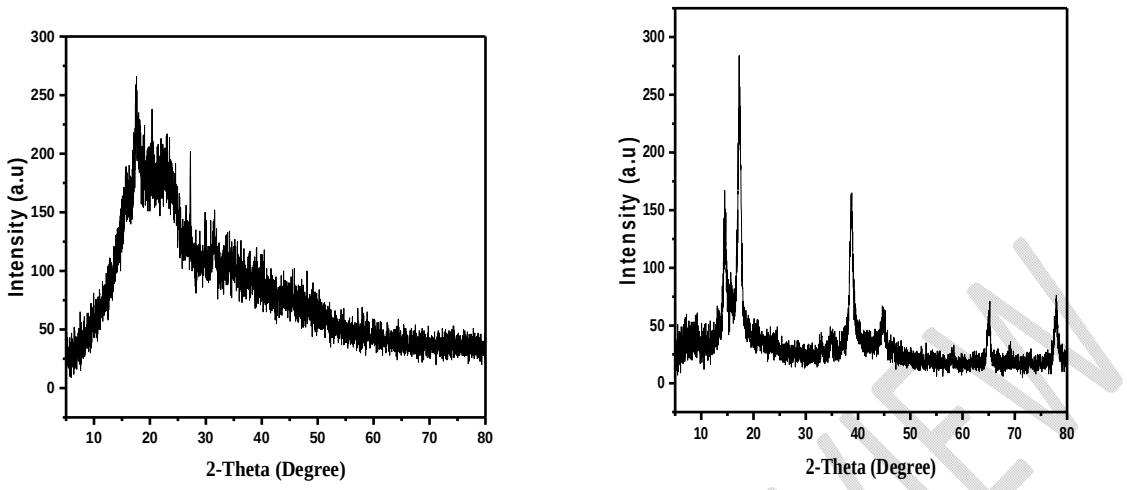

Fig3. XRD Spectroscopic Spectrum for avocado pear seed (APS)Fig 4. XRD Spectroscopic Spectrum for Silver Oxide nano-particle-Avocado Pear Seed (AgAPS)

3.3 SEM Charaterization

Scanning electron microscopy (SEM) was used to examine the surface morphology of the produced silver oxide nanocomposites at various magnifications. In contrast to avocado pear biomass, which is sparse and not as diagonally formed as those of AgAPS, the avocado pear seed nanocomposite (AgAPS) has similar rough surfaces, irregular surface structure, and hexagonal shape. The pictures show how the aggregation form of the silver oxide composite is forming an uneven surface structure. Zinc oxide nanoparticles made from CostusAfers leaf extract produced similar spectra (Chukwuemeka-okorie et al., 2023).

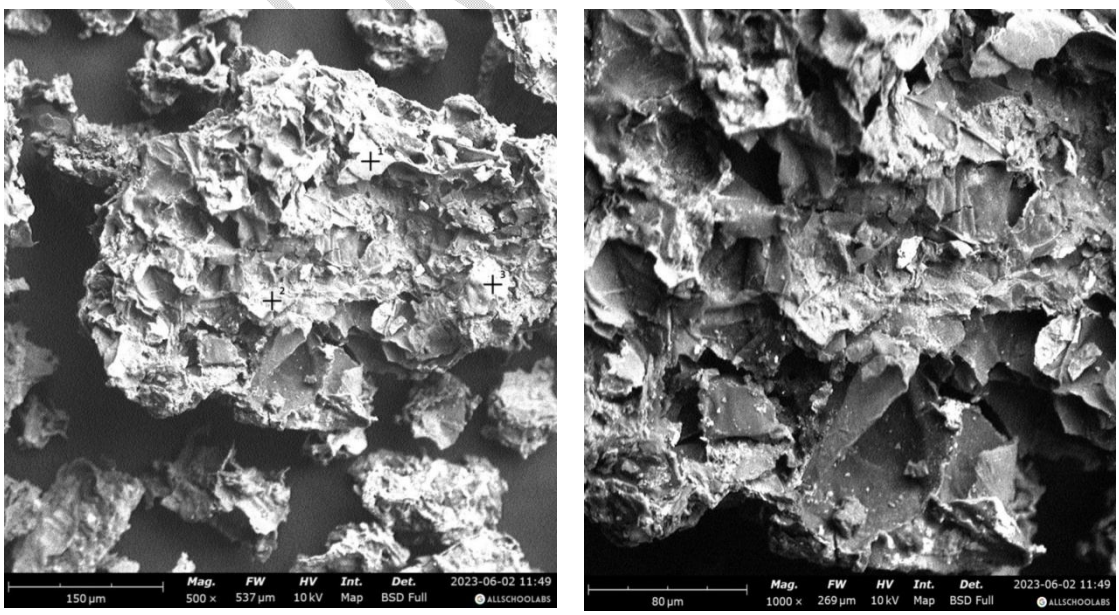

Fig 5-6. SEM **Spectrum of 500 and 1000 Mag for Silver Oxide nano-particle-Avocado Pear Seed (AgAPS)**

3.4 Effect of Time on Adsorption of Copper onto Avocado Pear Seed

Figure below displays the findings of the investigation into the impact of time on the adsorption of copper onto avocado pear seed (APS) and silver nanocomposite (AgAPS). The proportion of copper removed rose when the sorption duration increased from 30 to 180 minutes. The maximal adsorption capacity of the AgAPS was 29.3966 mg/g, and the APS was 28.1994 mg/g after 180 minutes. According to Dawodu and Akpomie (2014), the first rapid adsorption may have resulted from the material's surface adsorption followed by penetration into the inner tiny gaps. According to Nwadiogbu et al. (2016), the attachment-controlled process that results from a decrease in the number of sites available for active adsorption may be the source of the sluggish adsorption rate over time.The results showed the fast and stable nature of the process as only an insignificant difference was observed between the initial and final contact time (Hussein *et al*., 2006; Nwankwere*et al*., 2010). In all the time studied, AgAPS showed a higher adsorption capacity than APS. This might be due to enhanced active adsorption sites created by the presence of Ag molecules. The results obtained in this study are in agreements with reports elsewhere (Akpomie and Conradie, 2020).

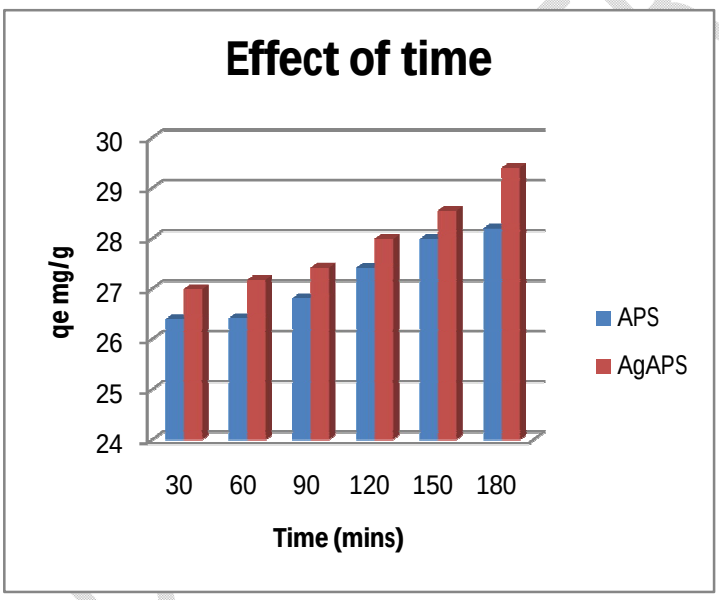

Figure 7. Effect of time on the adsorption of copper onto avocado pear seed

3.5 Effect of pH on the adsorption of copper onto avocado pear seed

In any adsorption investigation, the adsorbent and adsorbate species are impacted by the waste water's solution pH. This results in changes to the surface charge and speciation at different pH levels due to the protonation or deprotonation of the functional groups in both the adsorbent and the adsorbate

(Akpomieand Conradie, 2020). During the adsorption process, charged species may come into contact with one another via electrostatic interactions. As a result, solution pH is a crucial factor that influences adsorption and should be taken into account. The figure below displays the findings of the pH's impacts on copper's adsorption onto APS and AgAPS. The equilibrium sorption capacity was minimum at pH 2 (24.7965 and 24.8874mg/g) for APS and AgAPS respectively and reached a maximum at pH 10 (27.6342mg/g) for APS and pH 10 (28.1215mg/g) for AgAPS. The lower sorption capacity at low pH can be explained by the fact that at acidic pH, H^+ may compete with Cu^{2+} ions for the adsorption sites of the adsorbent, thereby inhibiting the adsorption of copper ions. Similar results are reported by (Hameed and El-Khaiary, 2018).

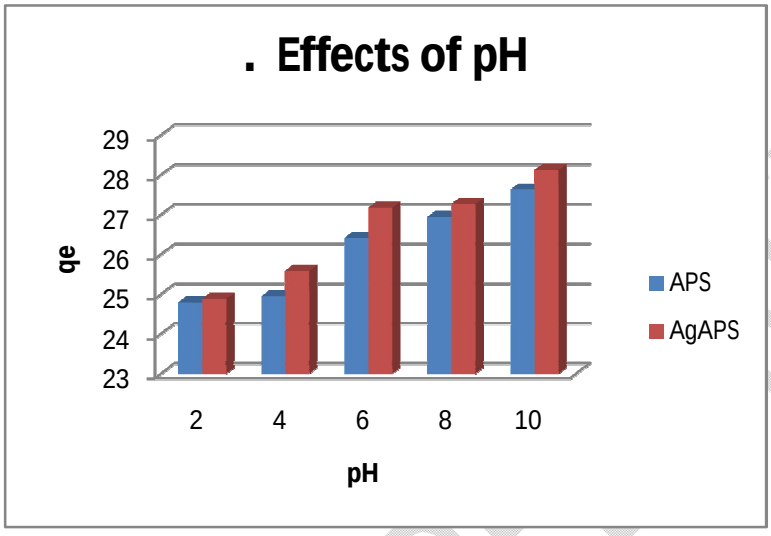

Figure 8. Effects of pH on the adsorption of copper onto avocado pear seed

3.6 Effect of Dosage on the Adsorption of Copper onto Avocado pear seed

One more significant and powerful factor influencing the adsorption process is the dosage of the adsorbent. Figure below shows the outcomes of the impacts of adsorbent dosage on copper adsorption onto APS and AgAPS. For APS and AgAPS, respectively, an increase in percentage removal between (88.0483 – 94.1900%) and (90.5850 – 95.3252%) was noted as the adsorbent dose increased from 0.1g to 0.5g. This could be explained by both the presence of active adsorption sites and a larger surface area (Zafar et al., 2006). Nevertheless, the opposite pattern was noted, as seen in the figure below, which illustrates how the adsorbent dose increased along with a reduction in adsorption capacity.

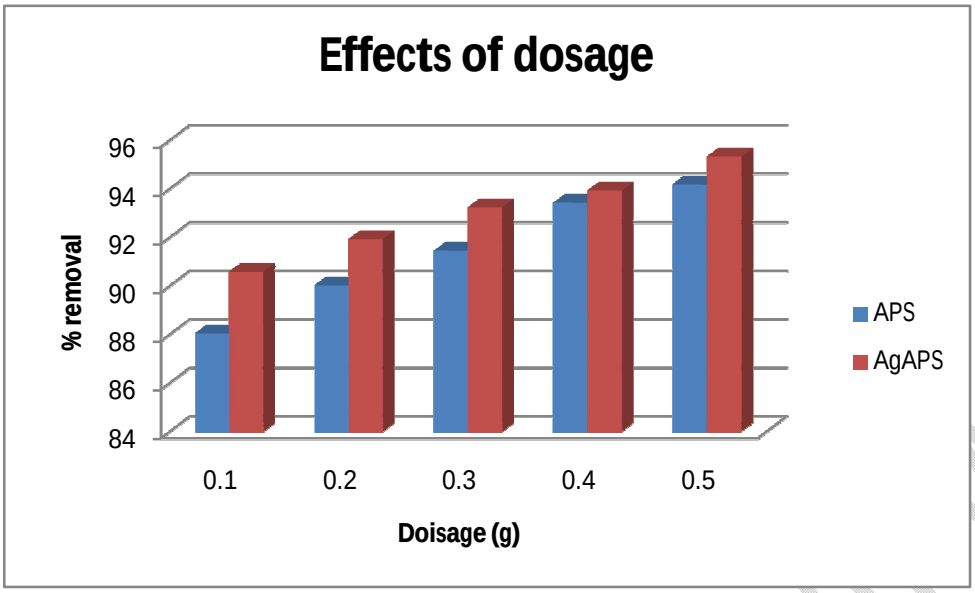

Figure .9. Effects of dosage on the percentage removal of copper onto avocado pear seed

3.7 Effect of Temperature on the Adsorption of Copper onto Avocado Pear Seed

The majority of contaminants' absorption from solution is also significantly influenced by the temperature of the effluent. In this context, the Figure below presents the findings of the investigation into the effects of temperature on Copper adsorption onto APS and AgAPS. The elimination of copper ions rose from 26.4145 mg/g to 28.5790 mg/g for APS and from 27.1756 mg/g to 28.9728 mg/g for AgAPS when the temperature was raised from 303 to 323 K. This suggested that the reaction process is endothermic and that higher temperatures favor the adsorption of copper ions onto both adsorbents (Akpomie and Conradie, 2020).The increase in the adsorption capacity may be as a result of the enhanced mobility of copper molecules with higher temperature for more interaction with the active sites of the adsorbent (Akpomie and Conradie, 2020b). It is also attributed to the creation of new active sites on the adsorbent surface, due to the removal of some surface impurities as the temperature increases (Akpomie and Conradie, 2020b).

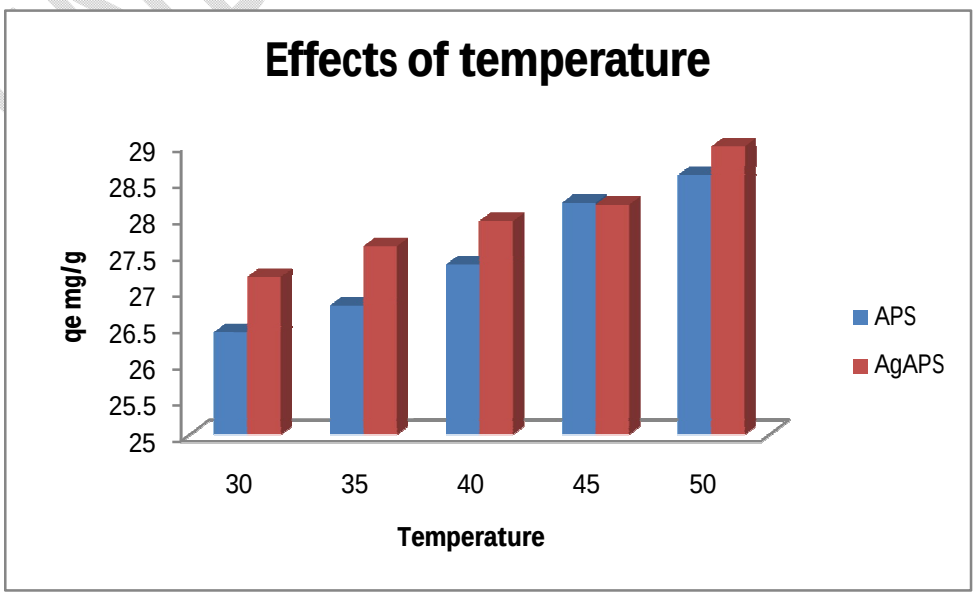

Figure 10. Effects of temperature on the adsorption of copper onto avocado pear seed

3.8 Kinetics of Copper adsorption onto Avocado Pear Seed

To explain the adsorption of copper onto APS and AgAPS, the experimental data were treated with pseudo first order kinetic model, pseudo second order kinetic model and intra-particle diffusion kinetic model. Plots for pseudo first order and pseudo second order kinetic models were presented respectively. The values of coefficient of determination R^2 for the pseudo second order model (0.999 and 0.999) fare higher than the pseudo first order model (0.904 and 0.890) for AgAPS and APS respectively, and also the estimated qe values from the pseudo second model were closer to the experimental values than the pseudo first order model. The goodness of fit and accurate prediction of qe both indicate that the pseudo second order model better describes the adsorption of copper onto APS and AgAPS and that chemisorptions is the likely mechanism of attraction (Akpomie and Conradie, 2020). A similar result was obtained in the adsorption of malachite green onto rattan saw dust (Hameed and Khaiary, 2008).Copper and other metal ions in solution can be transported from the aqueous phase to the surface of the adsorbent, and can as well diffuse into the interior of the porous particles (Nwadiogbu*et al*., 2016). It is expected that the plot of qe versus $t^{1/2}$ would give a linear relationship when intraparticle diffusion is involved in the mechanism of the biosorption process and that intraparticle diffusion would be then controlling mechanism if the line passed through the origin (Hill *et al*., 1998; Igwe and Abia, 2006). However, for the case where the plots do not pass through the origin, the reason has been suggested that intra-particle diffusion is not the only mechanism involved in the sorption process due to some degree of boundary layer control (Bulat *et al*., 2008). The intercept of the intra-particle diffusion model (25.55 and 24.81) for AgAPS and APS respectively, indicated that copper adsorption onto APS and AgAPS is by surface reaction and diffusion into the pores of the materials. This is in agreement with results from (Nwadiogbu*et al*., 2014; Akpomie and Conradie, 2020).

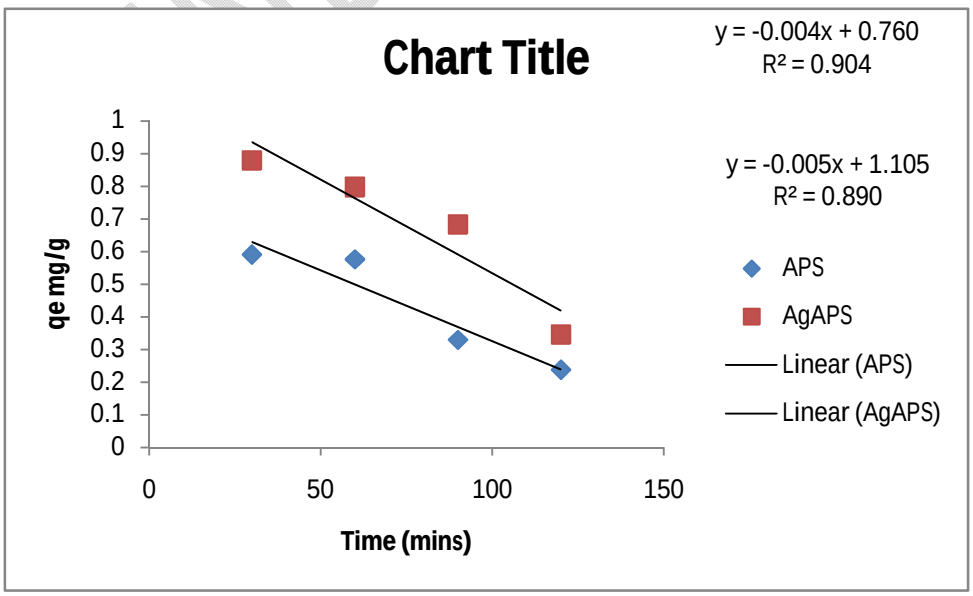

Fig 11 Pseudo first order kinetic plot for the adsorption of copper onto avocado pear seed

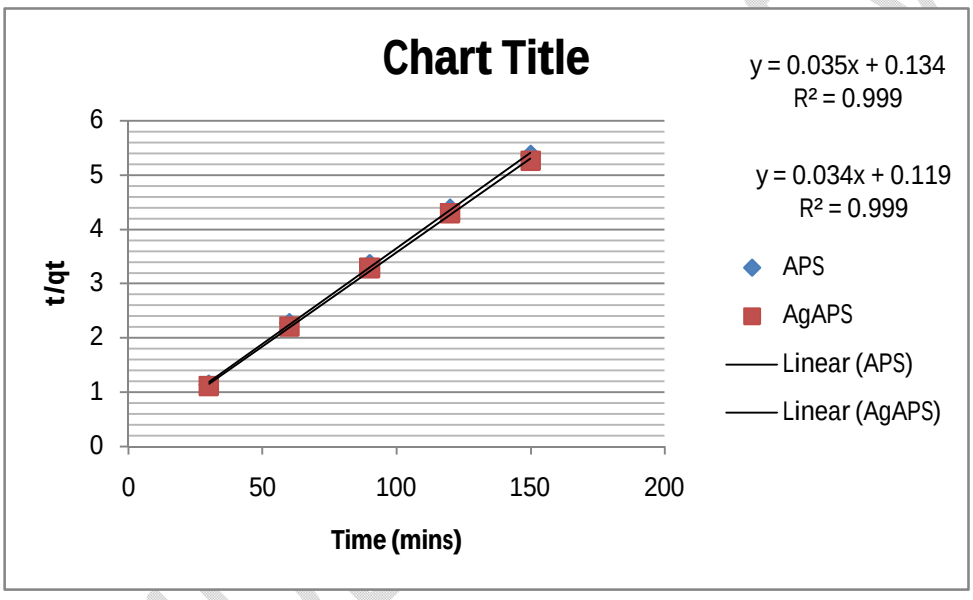

Fig 12 Pseudo second order kinetic plot for the adsorption of copper onto avocado pear seed

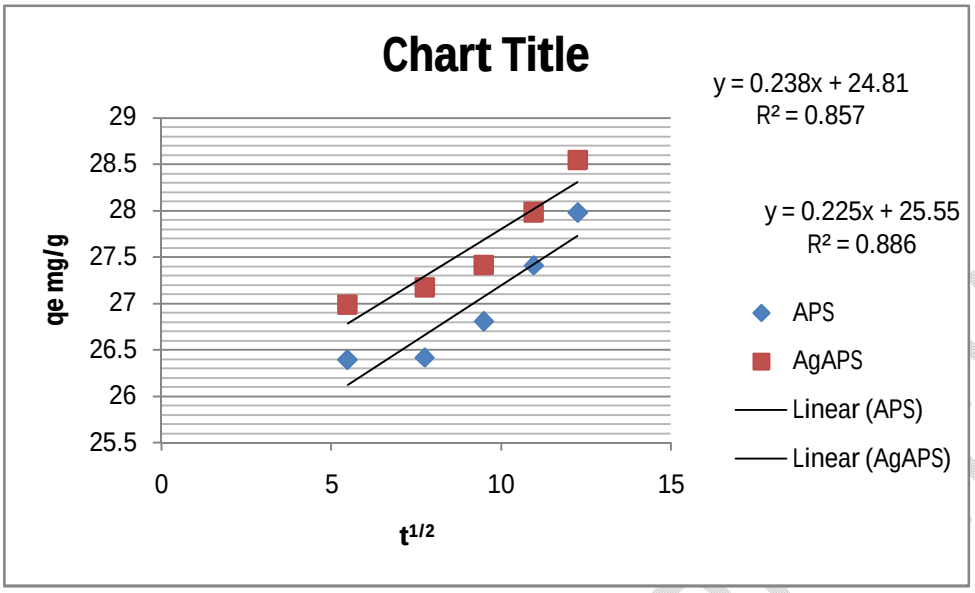

Figure 13. Intra-particle diffusion plot for the adsorption of copper onto avocado pear seed

3.9 Thermodynamics of Adsorption of Copper onto Avocado Pear Seed

The thermodynamic parameters; ΔH^o, ΔS^o and ΔG^o provides a very useful information on heat changes, spontaneity and randomness of the sorption process. The plot of lnK against temperature are presented in Figure 14 and the calculated thermodynamic parameters for the sorption of copper onto APS and AgAPS are presented below

Table 2-Thermodynamic parameters for the sorption of copper onto APS and AgAPS

	Cu APS	Ag APS
ΔH^0	0.4323	0.3991
ΔS^0	117.0611	105.0058
R^2	0.965	0.888

ΔG^0 303	-35,469.081	-31,816.358
308	-36,054.387	-32,341.387
313	-36,639.692	-32,886.416
318	-37,224.998	-33,391.445
323	-37,810.303	-33,916,474

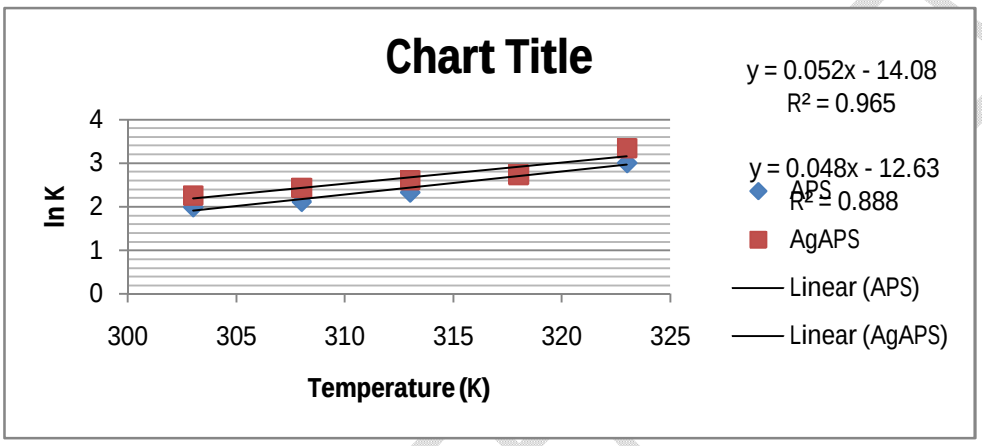

Fig 14 Thermodynamic plot for the adsorption of copper onto avocado pear seed

The positive value of ΔH^o values recorded for both APS and AgAPS indicated an exothermic removal of copper by APS and AgAPS, which correlates the increase in copper adsorption with temperature increase. The positive value of ΔS^o represents enhanced entropy on the solid-solution interface during the adsorption and development of structural changes, and thus irreversibility of the process (Somayeh *et al.*, 2019). The negative values of Gibbs free energy in all the temperatures studied, represents the spontaneity of the process (Somayeh *et al.*, 2019). Elevation in ΔG^o, with temperature enhances the extent of adsorption and at higher temperatures the metal ion becomes hydrated faster and its adsorption increases.

4.0 CONCLUSION

It was discovered that the copper ions in industrial waste water can be adsorbed by biosynthesized silver metal nanocomposite made from avocado peer seed. Atomic Absorption Spectroscopy (AAS) was used to investigate the equilibrium kinetics and thermodynamics for the removal of heavy metals utilizing the bio-synthesized nanocomposites. FTIR, XRD, and SEM were used to characterize the silver metal nanocomposite that were biosynthesized. For the sorption of heavy metals, equilibrium and kinetic models were created by taking into account the effects of dosage, temperature, initial pH, contact time, and initial concentrations of heavy metal ions. Avocado raw seed absorbed copper ions, but its silver metal nanocomposite increased the amount of adsorption. In comparison to the raw agricultural wastes,

the action of the adsorbent did demonstrate increased adsorption for the nanoparticles.The maximum percentage removal of copper ion was 92.2726% and 94.1900% for APS and AgAPS respectively.

REFERENCES

1. Adeyemi, O.O., Okpo, S.O., and Ogunti, O.O.,(2002). Analgesic and anti-inflammatory effects of the aqueous extract of leaves of Persea americana Mill (Lauraceae). *Fitoterapia.* 73(5):375–380.

2. Akpome, K. G. and Conradie. J. (2020).Efficient synthesis of magnetic nanoparticle-Musa acuminata peel composite for the adsorption of anionic dye. *Arab J. Chem.,* 13: 7115 – 7131.

3. Akpomie, K.G Panda Conradie, J. (2020b).Biogenic and chemically synthesized Solanum tuberosum peel-silver nanoparticle hybrid for the ultrasonic aided adsorption of bromophenol blue dye *Nature research*, 10: 17094.

4. Alexis, F., Pridgen, E., Molnar, L.K. and Farokhzad, O.C., (2008), Factors affecting the clearance and biodistribution of polymeric nanoparticles. Mol. Pharm. 5, 505–515.

5. Alhassan, A.J., Sule, M.S., Atiku, M.K.,(2012). Effects of aqueous avocado pear (Persea americana) seed extract on alloxan induced diabetes rats. Greener Journal of Medical Sciences 2(1):005–011.

6. Ali, A., Zafar, H., Zia, M., Ul-Haq, I., Phull, A.R., Ali, J.S. and Hussain, A., (2016), Synthesis, characterization, applications, and challenges of iron oxide nanoparticles.Nanotechnol. Sci. Appl. 9, 49–67.

7. Anaka, O.N., Ozolua, R.I., Okpo, S.O.,(2009). Effects of the aqueous seed extract of Persea americana mil (Lauraceae) on the blood pressure of spraguedawley rats. *African Journal of Pharmacy and Pharmacology.;*3(10):485–490.

8. Bulat, E., Ozacon, M and Segil, I.A., (2008). Adsorption of malachite green onto bentonite: equilibrium and kinetic studies and process design microprocessor mesoperons materials, 115: 234 – 246.
9. Chukwuemeka-okorie, H.O., Ani, J.U., Agbo, S.U., Odewole, O.A., Ojo, F.K., Alum, O.L., Akpomie, K.G., Ofomatah, A.C and Aralu, C.C.(2023). Adsorptive performance of green synthesized zinc oxide nanoparticles for the removal of cadmium (II) and lead (II) ions. *IOP Conf. Series: Earth and Environmental Science*. 1178: 012021
10. Dahiya, S., Tripathi, R.M. and Hegde, A.G., (2008), Bioresource Technology, 99: 129-187.
11. Dahiya, S., Tripathi, R.M. and Hegde, A.G., (2008), Bioresource Technology, 99: 129-187.
12. Dai, H., Huang, Y., Zhary, H., Ma, L., Huary, H., Wu, J and Zhang, Y. (2020) Direct fabrication of hiearachially processed pineapple peal hydrogels for efficient conjured adsorption. Carbohydrate polygon 280, 115599
13. Dawodu, F.A and Akpomie, K.G. (2014). Simultaneous adsorption of Ni(II) and Mn(II) ions from aqueous solution onto a Nigerian Kaolinite clay. *J. Mater. Res Technol.,* 3(2): 129-141.

14. Djeussi, D. E., Noumedem, J. A. K., Mihasan, M., Kuiate, J. R and Kuete, V. (2020). Antioxidant Activities of Methanol Extracts of Thirteen Cameroonian Antibacterial [Dietary] Plants. *Journal of Chemistry,* 1–13. DOI:https://doi.org/10.1155/2020/8886762
15. Dreaden, E.C., Alkilany, A.M., Huang, X., Murphy, C.J. and El-Sayed, M.A., (2012), The golden age: gold nanoparticles for biomedicine. Chem. Soc. Rev. 41, 2740–2779.

16. Egbuonu, A.C.C., Cpara, C.I and Atasie, OC.,(2017). Vitamins composition and antioxidant properties in normal and monosodium glutamate-compromised rats' serum of avocado pear (Pearsea americana) seed. Open Access Journal of Chemistry ;1(1):19–24.

17. Esumi, K., Tano, T., Torigue, K. and Meguro, K., (1993), Preparation and characterization of Biometallic Pd-Cu colloids by Thermal Decomposition of their Acetate Compounds in Organic Solvents, J. Phys. Chem B, 97, 5457-5471.
18. Hameed, B. H and El-khaiary, M.I. (2008). Malaite green adsoption by raw rathan dust, Isotherm, Kinetic and mechanism. *Journal of hazardous materials,* 159: 574 – 579.

19. He, Y, Wei, F, Ma, Z., Zhang, I., Yang, Q., YaO, B., Huang, Z., Li, J., Zeng, C and Zhang, Q. (2017). Green Synthesis of Silver nanoparticles using seed extract of Alpinia Katsumadai and their antioxidant, Cytotoxicity and anti-bacterial activities. *RSC Adv.,* 7: 39642 – 39851.

20. Hill, C.A.S., Jones, D., Strickland, G and Cetin, N.S. (1998). Kinetic and mechanistic aspects of the acetylation of wood with acetic anlydride.*Holzforschung,* 52: 623 – 629.

21. Huang, W. and Zhi-min, L., (2013) Colloids surf B., 105, 113-119.

22. Hua, M., Zhang, S. and Pan, B., (2012), Heavy metal removal from water/waste water by nanosized metal oxides: a review, J. Hazard. Mater, 211, pp.317-331.

23. Hussain, J.I., Kumar, S., Hashmi, A.A. and Khan, Z., (2001). Silver nanoparticles: preparation, characterization, and kinetics. Adv Matter Lett. 2(3): 188-194.

24. Igwe, J. C and Abia A.A. (2006). A bio separation process for remaining heavy metals from waste water using biosorbents. *African journal of Biotechnology,* 5: 1167 – 1179.

25. Laurent, S., Forge, D., Port, M., Roch, A., Robic, C., Vander Elst,L., and Muller, R.N., (2010), Magnetic iron oxide nanoparticles: synthesis, stabilization, vectorization, physicochemical characterizations, and biological applications. Chem. Rev. 110.

26. Liz – Marzan, L.M. and Lado – Tourina, I., (1996), Reduction and Stabilization of Silver Nanoparticles in Ethanol by Nonionic Surfactants. Langmuir, 12, 3585-3589.

27. Naveed, M., Bukhari, B., Aziz, T., Zaib, S., Mansoor, M. A., Khan, A. A., Shahzad, M., Dablool, A. S., Alruways, M. W., Almalki, A. A., Alamri, A. S and Alhomrani, M. (2022). Green Synthesis of Silver Nanoparticles Using the Plant Extract of Acer oblongifolium and Study of Its Antibacterial and Antiproliferative Activity via Mathematical Approaches. *Molecules,* 27(13), 4226. DOI:https://doi.org/10.3390/molecules27134226

28. Nwadiogbu, J. O., Okoye, P.A.C., Ajiwe, V.I.E and Nnaji, J.N. (2016). Removal of crude oil from aqueous medium by sorption on hydrophobic corncobs: Equilibrium and kinetic studies. *Journal of Taibah University for science*, 10(1):56-63.

29. Nwadiogbu, J. O. Okoye, P.AC., Ajiwe, V.I.E Nnaji J.N. (2014). Hydropholic treatment of corncob by acetylation. Kinetic and thermodynamic studies. 12(3)23-31.

30. Ojewole, J.A. and Amabeoku, G.J.(2006). Anticonvulsant effect of Persea americana Mill. (Lauraceae) (Avocado) leaf aqueous extract in mice. Phytother Res. 20(8):696–700.

31. Pileni, M.P., (2001), Fabrication and Physical Properties of Self-organized Silver Nanocrystals. Pure Applied Chem. 72, 53-65.

32. Radhakrishnan, A., Rejani, P. and Beana, B., (2015), CuD/Polypyrole nanocomposites as a marker of toxic lead ions for ecological remediation in contrast with CuO and polypyrrole main group met. Chem. 38 (5-6): 133-143.

33. Somayeh, R., Albas, R., Muhammed, N.Z., Syed, S.S and Shahin, A. (2019). Synthesis and characterization of MgO supported Fe-Co-Mn nanoparticles with exceptionally high adsorption capacity for Rhodamine B dye.*Journal of Materials Research and Technology,* 41:2238 – 2249.

34. Ventura, L.M.B., Mateus, V.L., De Almeida, A.C.S.L., Wanderley, K.B. and Taira, F.T., (2017). Chemical composition of fine particles (PM 2.5): water soluble organic fraction and trace metals. Air Quality, Atmosphere and Health Journal. 10(7):845-852.